Effects of Constraint Release on the Dynamics of Entangled Linear Polymer Melts

Jean-Pierre Montfort,* Gérard Marin, and Philippe Monge

Laboratoire de Physique des Matériaux Industriels, Université de Pau et des Pays de l'Adour, 64000 Pau, France. *Received July 20, 1983*

ABSTRACT: The mechanism of constraint release for an entangled linear chain of polystyrene diffusing by reptation is emphasized, dissolving large N chains in a matrix of shorter N_s chains of the same species. Dynamic shear measurements allow us to define an average relaxation time $\bar{\tau}(N,N_s)$ for the relaxation of the large chains, from which we derive another average relaxation time $\bar{\tau}_{mod}(N,N_s)$ for the tube modification induced by constraint release. We find that, according to the Klein and Graessley theories, the tube could be considered as a Rouse chain ($\bar{\tau}_{mod}(N,N_s) \propto N^{1.9\pm0.1}$) but constraint release is not directly connected to the reptation of the N_s chains ($\bar{\tau}_{mod}(N,N_s)^{2.3\pm0.1}$). The process of constraint release included in the diffusion of chains in a binary blend at various component concentrations allows us to specify the idea of "cell" in the Graessley theory and to describe reasonably the variations of the limiting parameters η_0 and J_e^0 with blend composition.

Introduction

The viscoelastic properties of entangled molecules are well described, for the slowest relaxation processes, by assuming they relax by diffusion along their own contours among topological obstacles. This process, called reptation, was introduced by de Gennes[1] and developed by Doi and Edwards.[2] The topological constraints, due to the fact that the molecules cannot pass through each other, confine each chain inside a tubelike region. The center line of such a tube is called the primitive path or the primitive chain, playing a role similar to the Rouse chain. The primitive chain is a freely jointed chain with N steps of length a corresponding to the breadth of the tube and corresponding to a correlation length ξ. The real chain is wriggling around the primitive chain but this wriggling motion occurs rapidly[1] and its magnitude is small, less than a. Thus, the large-scale motion of a real chain is a sliding motion along the primitive path through the network of other entangled chains. For monodisperse linear polymer melts, the diffusion coefficient D_G of the center of mass is proportional to N^{-2} and the characteristic relaxation time τ_d to N^3 as was first predicted by de Gennes.

The constitutive equations derived by Doi and Edwards, using the model of the primitive chain and applied to different rheometrical flows, agree qualitatively well with experiments (except for the first normal stress in the transient shear flow): in particular, the plateau modulus G_N^0 and the steady-state compliance J_e^0 are independent of chain length. But other predictions are slightly inconsistent with experiment: the theoretical value of the product $G_N^0 J_e^0$, which is constant for linear monodisperse polymers, is smaller than the experimental value by a factor of about 2.5, the viscosity varies more rapidly with chain length than predicted ($\eta_0 \propto M^3$ for the theory and $\eta_0 \propto M^{3.4}$ for experiments), and the theoretical effect of molecular weight distribution on steady-state viscosity and compliance is much stronger than the observed dependence for high molecular weight components.

These differences mean that other mechanisms may also play a role in the whole motion of the molecules. Klein[3] proposes a self-consistent model for the renewal of tube configuration, considering that the neighboring chains forming the tube reptate too inside their own tube. Each tube constraint is renewed with a characteristic time $\tau_R \propto N^2\tau_{rep} \propto N^5$ ($N = M/M_e$), M_e being the average weight between entanglements. For the highest molecular weight, $\tau_R \gg \tau_{rep}$, so reptation should be the dominating mechanism. Graessley[4] suggests that other transverse motions could occur. For example, a chain could "leak" from its tube anywhere along its length by projecting loops out through the surroundings, altering the tube length. Some experimental results suggest that the reptation is probably only one of the mechanisms operating in nonnetwork systems. Thus, the relaxation time of long unattached chains in a network is longer than in the corresponding monodisperse system,[5-7] the longest relaxation times of unattached star molecules in a network are very much larger than those in the homologous melt,[5] and, unlike the behavior of linear chains, the ratio of relaxation times appears to increase rapidly with arm length for star molecules.

Recently, Graessley[8] developed a model that predicts the effects of two sorts of motions: disengagement by fluctuations in path length and constraint release. The first, called "tube leakage", consists of a variation of the tube length from fluctuations in the path and surplus segment population of an unattached chain. This mechanism should be negligible for very long linear molecules. The second process is the effect of the motion in the surroundings on the relaxation of each chain. The neighbors exert the topologic constraints constituting the tube but these constraints have finite lifetimes. Every such constraint is released when the neighboring chain abandons the particular step along its own primitive path which provides the constraint. A local displacement of the path can then occur. Thus, this effect is strongly connected to the length of chains forming the matrix. The surroundings would be represented by a regular lattice of independently reptating chains. A chain with N path steps occupies N cells of the lattice. Each cell is bounded by z_0 strands of neighboring chains, occupying their own set of primitive path steps. These bars disappear and form again continually. Their lifetimes correspond to the lifetimes of primitive path steps which are at random locations along the neighboring chains. Graessley postulated that such a jump will not alter the path length, the local jump distance is the path step length a, and the average time between jumps is $2\tau_w$, where τ_w is the mean waiting time for release of a constraint. The average number of constraints per cell involving such a jump is z ($z < z_0$) and then, the mean waiting time is

$$\tau_w = \int_0^\infty [F(t)]^z \, dt = \Lambda(z)\tau_d \qquad (1)$$

where

$$F(t) = \frac{8}{\pi^2} \sum_{n \text{ odd}} \frac{1}{n^2} \exp(-n^2 t/\tau_d)$$

0024-9297/84/2217-1551$01.50/0

Table I
Molecular and Rheological Properties of Linear Polystyrenes at 160 °C

sample	M_w	P	η_0, P	J_e^0, cm²/dyn	$\eta_0 J_e^0$	$\bar{\tau}$, s
F04	35 000	1.06	3.02×10^4	4.00×10^{-7}	1.2×10^{-2}	1.48×10^{-2}
F10	100 000	1.06	5.75×10^5	1.26×10^{-6}	7.24×10^{-1}	5.75×10^{-1}
F11	110 000	1.05	7.94×10^5	1.25×10^{-6}	1.00×10^0	7.58×10^{-1}
F20	200 000	1.06	6.03×10^6	1.38×10^{-6}	8.32×10^0	5.01×10^0
F39	390 000	1.10	4.36×10^7	1.58×10^{-6}	6.92×10^1	4.00×10^1
F90	900 000	1.12	6.92×10^8	2.09×10^{-6}	1.44×10^3	1.00×10^3
F120	1 200 000	1.2				
F270	2 700 000	1.2	1.59×10^{10} [a]	3.16×10^{-6}	5.01×10^4	4×10^4 [a]
F380	3 800 000	1.3				

[a] These values have been extrapolated from measurements between 210 and 250 °C.

is the fraction of all initial steps still occupied at time t, and

$$\Lambda(z) = \frac{1}{z}\left(\frac{\pi^2}{12}\right)^z$$

Graessley demonstrates that the constraint release contribution to the diffusion of the center of gravity of a linear chain is

$$D_G = a^2/(12N\tau_w)$$

If constraint release were the only process for conformational rearrangement, the initial path motions would be the same as the chain motions of the N-element Rouse model. Thus, the longest relaxation time for constraint release would be

$$\tau_{r1} = \frac{\langle R^2 \rangle}{6\pi^2 D_G} = \frac{2}{\pi^2}\Lambda(z)N^2\tau_d \qquad (2)$$

Assuming that no correlation occurs in the effects of simultaneous reptation and constraint release, Graessley derived an expression for the steady-state viscosity like $\eta_0 = G_N^0 \bar{\tau}_n$, where $\bar{\tau}_n$ is an average relaxation time of the terminal region. For a monodisperse linear polymer, Graessley obtains

$$\bar{\tau}_n = \frac{8}{\pi^2 N}\sum_{i\ \mathrm{odd}}\sum_{j=1}^{N}\frac{1}{i^2}\left(\frac{i^2}{\tau_d} + \frac{N^2\lambda_j}{\pi^2\tau_{r1}}\right)^{-1}$$

with

$$\lambda_j = 4\sin^2\left(\frac{\pi j}{2(N+1)}\right)$$

and Klein[3] postulates that

$$\frac{1}{\tau} = \frac{1}{\tau_d} + \frac{1}{\tau_{r1}}$$

which is a form similar to the above equation for $i = 1$ and $\lambda_j = \lambda_1$.

For the two authors, $\tau_{r1}/\tau_d \propto N^2$ indicates that, for a monodisperse linear polymer, reptation is the outstanding process. But, the waiting time τ_w depends on the nature of the surroundings. If the diffusing species occupies N steps in a matrix of linear chains with N_s steps, then

$$\tau_w(N,N_s) \propto \tau_d(N_s) \qquad (3a)$$

and

$$\tau_{r1}(N,N_s) \propto N^2 N_s^3 \qquad (3b)$$

If $N_s \ll N$, $\tau_{r1}(N,N_s)/\tau_d(N) \propto N_s^3/N$ and the constraint release will contribute to the diffusion of the N chain in a matrix of shorter N_s chains.

Daoud and de Gennes[9] consider also a "tube renewal" process for one long chain in a monodisperse melt of shorter chains of same species and they show that the diffusion constant $D_{ren}(N)$ for the test chain should be

$$D_{ren}(N) \propto N^{-1}N_s^{-3}$$

which leads to a corresponding relaxation time $\tau_{ren}(N) \propto L^2/D_{ren}(N) \propto N^2N_s^3$ like eq 3.

These authors postulate that both reptation and tube renewal must break down when the N chain becomes extremely long, the test coil moving like a hydrodynamic sphere in a continuous medium.

In this paper, we discuss the effect of constraint release on the terminal relaxation of large linear chains included in a matrix of shorter linear chains of the same chemical nature (polystyrene). In part I, we describe the experimental method used to determine an average relaxation time of the large chains, using periodic shear flow. In part II, we give results showing the influence of the matrix (N_s chains) and of the individual N chain on the variations of the average time of constraint release for the large chain. Then we emphasize the effect of the large chain concentration in the surroundings on the average relaxation time of the two components of the binary blends. We will derive from that study an equation for the zero-shear viscosity η_0 and the steady-state compliance J_e^0 for binary blends of monodisperse linear polymer melts, including the effects of constraint release.

I. Experimental Section

1. Samples. We have used fractions of linear polystyrene manufactured by Pressure Chemical Co. Their main features are listed in Table I. The samples, fractions and binary blends, were prepared in the following way. They were dissolved in benzene at a concentration of about 0.03 g cm^{-3} with a very small amount of antioxidant (Dionol at 0.1% by weight) and freeze-dried in liquid nitrogen under a vacuum of about 2–3 mm of mercury for 30–40 h at room temperature. The samples were then vacuum-molded at about 200–230 °C as small disks with a diameter of 2 cm and a thickness of 2 mm.

2. Experimental Technique. The dynamic shear measurements were performed with an Instron 3250 rheometer. The sample is sheared between cone and plate. The radius of the plate is 1 cm, the angle of the cone being 7.5°. The frequency of the upper cone oscillation may be varied between 10^{-3} and 10^{+2} Hz, the oscillation amplitude decreasing with frequency so the shear strain is lower than 0.02. Data for the entrance signal is provided by a Hewlett-Packard 9845B computer to a Schlumberger frequency analyzer–generator, which generates the signal driving the motor.

The exit signal, corresponding to the torque applied to the lower plane, is returned to the analyzer, which compares the two signals, amplitude, and phase. The amplitude ratio and the phase angle are transmitted to the computer (Figure 1). Thus, it calculates the dynamic storage modulus $G'(\omega)$, the loss modulus $G''(\omega)$, the

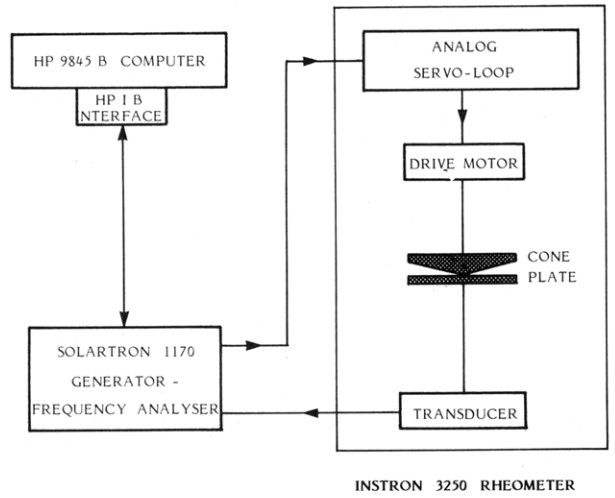

Figure 1. Block diagram of the experimental setup.

dynamic viscosity $\eta'(\omega) = G''(\omega)/\omega$ and its imaginary part $\eta''(\omega) = G'(\omega)/\omega$, and the storage compliance $J'(\omega) = G''(\omega)/|G^*(\omega)|^2$.

The experiment is entirely automated in the whole frequency range. The sample temperature may be selected from room temperature to about 300 °C with a stability of 0.1 °C. The accuracy is better than 5% for the dynamic data.

Measurements were made between 160 and 250 °C for all samples, fractions and blends. For the very long chains ($M >$ 900 000), we changed the sample at each temperature and, after each experiment, we checked again the data at the lowest frequencies, in order to make sure that the sample had not degraded. This check was made also by measuring molecular weights after the experiments by gel permeation chromatography but this was inefficient for the blends containing only 2% of long chains.

We have constructed the master curves for $G'(\omega)$ and $G''(\omega)$ for each sample, using a horizontal shift factor $a_T = \eta T_0 \rho_0 / \eta_0 T \rho$ for the terminal region and the onset of the transition region.[16] A vertical shift factor is not required for the terminal region because the steady-state compliance J_e^0 seems independent of the temperature for $1.2 < T/T_g < 2$.[11] Thus, the average relaxation times are shifted, at different temperatures, by the same shift factor a_T, which is, within experimental uncertainties, the same for all the fractions and blends studied. The reason for this is that, for high molecular weight polymers, the free-volume fraction and so the mobility of the chains are practically independent of the molecular weight. For our experimental results, we have obtained $\log a_T = (704/T - 48.6) - 6.32$ with a reference temperature $T_0 = 160$ °C.

3. Determination of Terminal Average Relaxation Times. Formally, one can calculate the relaxation time distribution function $H(\omega)$ using Fuoss and Kirkwood formulas[12]

$$H\left(\tau = \frac{1}{\omega}\right) = \pm\frac{1}{\pi} I_m G^*(\omega e^{\pm i\pi})$$

if one knows an analytical formula for the complex shear modulus $G^*(\omega)$. Generally, this is not the case and thus, approximation methods[13-15] are used. But, we have demonstrated[16] that they provide rough results for monodisperse polymers. In particular, the longest time is underestimated and the overshoot of the spectrum in the terminal region is smoothed.

For high molecular weight fractions, Marin[17] has given an analytical expression for the complex compliance:

$$J^*(\omega) = J_\infty + \frac{1}{j\omega\eta_0} + \frac{J_p}{1 + (j\omega\tau_p)^{1-\alpha}} + \frac{J_t}{1 + (j\omega\tau_t)^{1-\beta}}$$

with a retardation time distribution of Cole and Cole[18] for the two retardation domains. J_p^* defines a terminal region associated with the whole motions of the chains.

The retardation time $\tau_p \propto M^{3.34}$ is similar to the disengagement time τ_d, and α is related to the breadth of the relaxation time distribution, which is in turn a function of the breadth of the molecular weight distribution. J_t^* is independent to the length

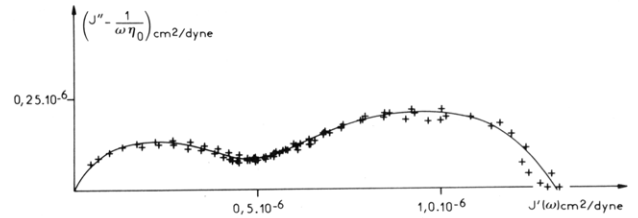

Figure 2. Retardational complex compliance for sample F39 at several temperatures: experimental data from ref 17 and full line from the analytical expression of $J^*(\omega)$ in the text.[17]

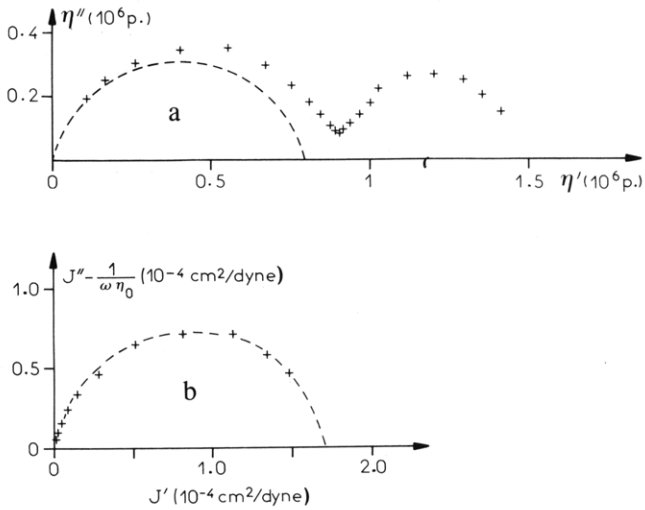

Figure 3. Dynamic properties in the terminal region for the blend F11–F270 with ϕ (weight fraction of the F270 sample) = 0.02 at 160 °C. From the master curves of $G'(\omega)$ and $G''(\omega)$, we deduce (a) the complex viscosity $\eta^*(\omega)$ and (b) the retardational compliance $J^*(\omega) - 1/j\omega\eta_0$.

and characterizes the motions of chain portions corresponding to the lengths between entanglements. Figure 2 shows the good agreement between the experiment and the given analytical expression. Thus, one can calculate the retardation spectrum

$$L\left(\tau = \frac{1}{\omega}\right) = \pm\frac{1}{\pi} I_m J^*(\omega e^{\pm i\pi})$$

and deduce the relaxation spectrum $H(\tau)$. This method is successful for monodisperse linear polymers. But, in the case of blends containing 2% of long chains, it is not possible to separate the various retardation domains, as shown in Figure 3b. Thus, it is difficult to derive an analytical expression for $J^*(\omega)$ showing the various contributions and, in particular, that of the long chains in a matrix of shorter chains. We cannot derive then the terminal relaxation times of the long chains in those blends with that method.

We can also determine the average relaxation times $\bar{\tau}_n$ and $\bar{\tau}_v$, which may be expressed as functions of the relaxation time distribution moments by[19]

$$\bar{\tau}_n = \frac{\int_{-\infty}^{+\infty} \tau H(\tau)\, d \ln \tau}{\int_{-\infty}^{+\infty} H(\tau)\, d \ln \tau} = \eta_0 / G_N^0$$

and

$$\bar{\tau}_v = \frac{\int_{-\infty}^{+\infty} \tau^2 H(\tau)\, d \ln \tau}{\int_{-\infty}^{+\infty} \tau H(\tau)\, d \ln \tau} = \eta_0 J_e^0$$

The ratio $\bar{\tau}_v/\bar{\tau}_n = G_N^0 J_e^0$ is a measure of the breadth of the relaxation spectrum and practically the same value $G_N^0 J_e^0 \simeq 3.0 \pm 0.5$ is found for different species of narrow-distribution polymers.[20]

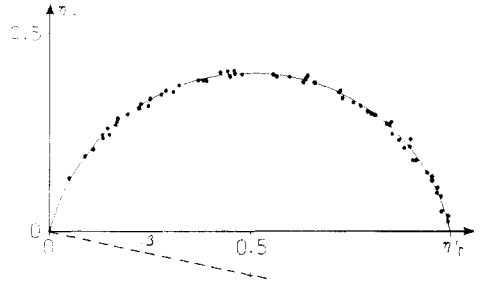

Figure 4. Reduced complex viscosity curves for several narrow-distribution samples: F04, F10, F11, F20, F39, and F90.

Experimentally, the parameters η_0 and J_e^0 are obtained by the standard formulas[10]

$$\eta_0 = \lim_{\omega \to 0} (G''/\omega)$$

and

$$J_e^0 = (1/\eta_0^2) \lim_{\omega \to 0} (G'/\omega^2)$$

So, we can calculate $\bar{\tau}_v$. But, this relaxation time includes all the terminal relaxation mechanisms, for both the matrix and the isolated N chains. As we need only an average terminal relaxation time for the N chains, $\bar{\tau}_v$ does not fit.

It is often difficult to get the plateau modulus G_N^0. According to Ferry's equation[10]

$$G_N^0 = \frac{2}{\pi} \int_{-\infty}^{+\infty} G''(\omega)\, \mathrm{d} \ln \omega$$

with only the terminal region contribution. It has been shown[21] that $G_N^0 \propto G_m''$, G_m'' being the maximum of the terminal loss modulus. But, this maximum is obtained only when the terminal and transition relaxations are well separated. For blends containing 2% of long chains, the terminal relaxation region of the long chains overlaps the terminal relaxation region of the matrix and the maximum of G'' is not observed in the low-frequency region, as shown in Figure 9. Thus, it is not possible to use the relaxation time $\bar{\tau}_n$.

Figure 3a shows that, if we represent the imaginary part of the complex viscosity $\eta''(\omega)$ vs. the dynamic viscosity $\eta'(\omega)$ for the blends, two terminal relaxation domains appear. The high-frequency domain represents the relaxation of the matrix because its amplitude is very similar to that of the N_s homopolymer, and Figures 8 and 9 show that the variations of G' and G'' in that region are very close to those of the N_s homopolymers. Thus, the low-frequency domain depicts the relaxation of the long N chain. In Figure 3b, the curve representing the retardational compliance $J^*(\omega) - (1/j\omega\eta_0)$ does not allow us to conclude whether the relaxational domain observed is characteristic either of the long chain or the whole blend. So, we have chosen the first representation ($\eta^*(\omega)$) to determine an average relaxation time of the long chain. For homopolymers, whatever the molecular weight distribution, we have shown[22] that the reciprocal of the frequency at the maximum of η'' represents an average relaxation time $\bar{\tau}$. Figure 4 shows a master curve for the reduced complex viscosity $\eta_r^*(\omega) = \eta^*(\omega)/\eta_0$ for narrow-distribution fractions of polystyrene. The value of the angle β is related to the breadth of the relaxation time distribution. Columns 6 and 7 of Table I show that $\bar{\tau}$ represents well an average terminal relaxation time because, for monodisperse linear polystyrene samples with a constant entanglement concentration (M/M_e greater than about 6), the ratio $\bar{\tau}_v/\bar{\tau} = 1.5 \pm 0.2$ and so $\bar{\tau}_n < \bar{\tau} < \bar{\tau}_v$.

Thus, we used this way of obtaining an average relaxation time of long N chains included in a matrix of shorter N_s chains, employing the low-frequency domain observed in the Cole–Cole plot of complex viscosity. The accuracy of $\bar{\tau}$ is about 10%.

II. Results and Discussion

1. Fractions. The variations of the limiting parameters η_0, J_e^0, and $\bar{\tau}$, for the fractions studied, follow the usual law as a function of molecular weight M: $\eta_0 = 5.4 \times 10^{-11} M^{3.2}$ (Figure 5), $\bar{\tau} = 5.25 \times 10^{-18} M^{3.4}$ (Figure 6) for $M > M_c \simeq 2M_e$, and $J_e^0 \propto M^0$ (Figure 7) for $M > 6M_e$, but J_e^0 increases with polydispersity. It should be observed

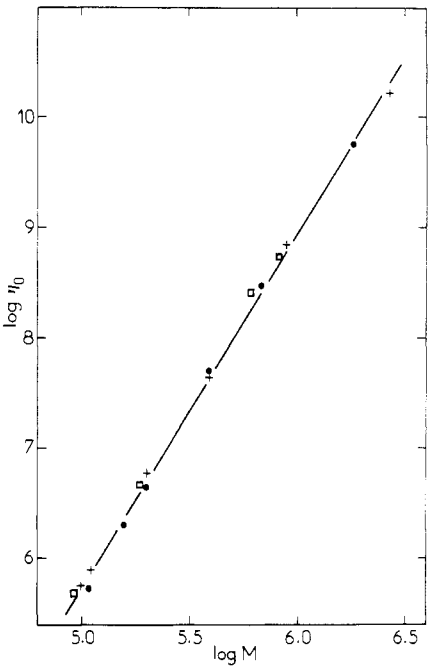

Figure 5. Zero-shear viscosity as a function of molecular weight at $T = 160$ °C for narrow-distribution samples: (+) data listed in Table I; (●) data from ref 17; (□) data from ref 30.

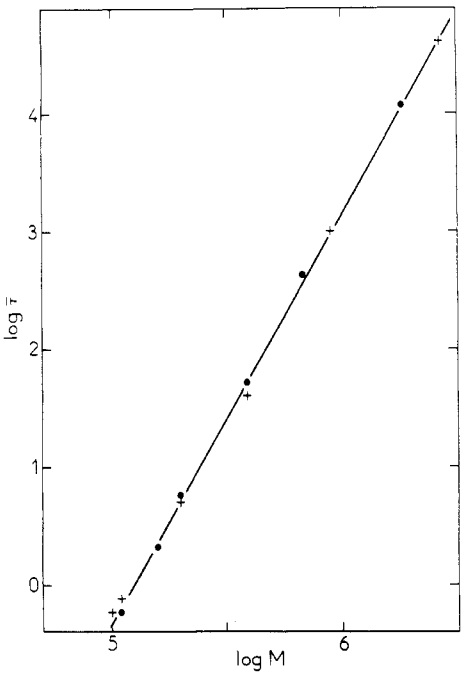

Figure 6. Average relaxation time as a function of molecular weight at $T = 160$ °C for narrow-distribution samples. The symbols have the same meaning as in Figure 5.

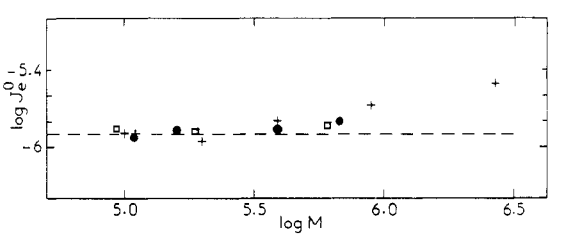

Figure 7. Steady-state recoverable compliance as a function of molecular weight for narrow-distribution samples. The symbols have the same meaning as in Figures 5 and 6.

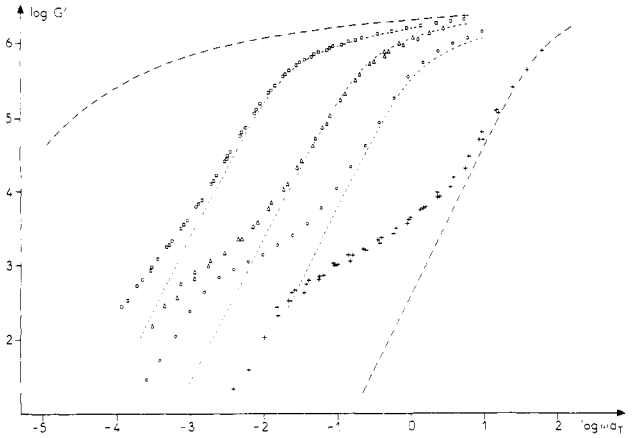

Figure 8. Master curves of storage modulus at $T = 160$ °C for the blends listed in Table II ($\phi = 0.02$). The dashed lines represent the behavior of fractions; from left to right: F270, F39, F20, F11, and F04.

that sample F270 has been studied between 210 and 250 °C, and the values of η_0 and $\bar{\tau}$ have been extrapolated at 160 °C using the shift factor a_T.

The relaxation time $\bar{\tau}$ is a measure of the diffusion motion of the chains in their own surroundings. The mechanisms involved may be reptation, constraint release, or tube fluctuation breakage. The latter will not be considered because this influence is negligible for chains[8] sufficiently long. Thus, if we consider only reptation and constraint release and assume that the two mechanisms are uncorrelated, we have

$$\frac{1}{\bar{\tau}} = \frac{1}{\bar{\tau}_{rep}} + \frac{1}{\bar{\tau}_{mod}} \tag{4}$$

with $\bar{\tau}_{rep}$ similar to the tube disengagement time τ_d and $\bar{\tau}_{mod}$ a tube modification time such as an average time of the tube motions in an N-element Rouse model (τ_{r1} would be the longest relaxation time of the tube).

For a monodisperse linear polymer, following Graessley's model, $\bar{\tau}_{mod}(N)/\bar{\tau}_{rep}(N) \simeq N^2$, so the reptation would be dominant for the high molecular weights.

2. Influence of the Matrix. In order to modify entirely the surroundings of the N chain, it was "isolated" in a matrix of shorter N_s chains of the same species (fractions of linear polystyrene). We have made blends of sample F270 in matrices F04, F11, F20, and F39, so $7 < M/M_s \sim N/N_s < 77$. The weight fraction of the N sample is 2% for the four blends, corresponding to a concentration of $C \simeq 0.02$ g/mL. In a solution, a macromolecule exhibits the behavior of an individual chain until the coils overlap or at least until there is an overlap of the hydrodynamic spheres of individual molecules for $C = C^* = M/N_A R_S^3$, where N_A is Avogadro's number and R_S Stokes' radius. For polystyrene in a good solvent $C^* \simeq 6 \times 10^{-3}$ g/mL at $M = 2\,700\,000$ (sample F270) from measurements using dynamic light scattering.[23] Each N chain in a melt of identical chains is Gaussian and ideal. But, in a matrix of N_s chains, the N chain stays ideal only up $M_s \simeq M^{1/2}$.[24] So, in our case, we can assume that all the blends studied are ideal and the N chain conformation is the same that in a Θ-solvent with $C_\Theta^* > C^*$. The real values of C^* and C_Θ^* are difficult to determine because they depend on the range of the interactions and thus on the definition of the radius R. For static effects, a radius of gyration R_G is used; for dynamic effects, a hydrodynamic radius R_H is used. So, we assume that, for the concentration $C = 0.02$ g/g, the interactions N–N are negligible. This assumption will be confirmed in part II-4 of this paper, where the Figure 17 shows that the average tube modification time $\bar{\tau}_{mod}$ is practically independent of the concentration for $C \leq 0.02$ g/g.

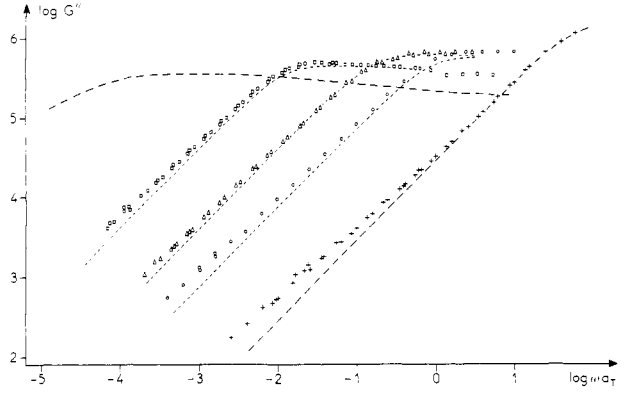

Figure 9. Master curves of loss modulus at $T = 160$ °C for the blends listed in Table II ($\phi = 0.02$). The dashed lines have the same meaning as in Figure 8.

Table II
Relaxation Times of N Chains in N_s Matrices at 160 °C

N chain	N_s matrix	$\bar{\tau}(N,N_s)$, s	$\bar{\tau}_{mod}(N,N_s)$, s
F270	F04	3.5×10^1	3.5×10^1
F270	F11	7.8×10^2	7.95×10^2
F270	F20	1.6×10^3	1.7×10^3
F270	F39	1×10^4	1.3×10^4
F270	F270	4×10^4 [a]	1.2×10^6 [b]

[a] This value has been extrapolated from measurements between 210 and 250 °C. [b] This value has been extrapolated from the straight line in Figure 10.

Figures 8 and 9 show the variations of storage modulus $G'(\omega)$ and loss modulus $G''(\omega)$ vs. the molecular weight M_s of the matrix. Two domains can be distinguished: the high-frequency domain has been superposed, with the dashed line representing the behavior of the matrix alone (obtained from the homopolymer data), and so represents the contribution of the matrix to the terminal relaxation processes; the low-frequency domain is due to the presence of the long chain. Starting from the master curves of $G'(\omega)$ and $G''(\omega)$, we have calculated $\eta'(\omega)$ and $\eta''(\omega)$ and deduced the average relaxation time $\bar{\tau}(N,N_s)$ of an N chain in an N_s matrix. If we assume that the relaxation time measured for the homopolymer is only a reptation time $\bar{\tau}_{rep}(N)$ (F270 is a sample with very long chains), we can deduce the average time of tube modification $\bar{\tau}_{mod}(N,N_s)$ from a relation similar to relation 4:

$$\frac{1}{\bar{\tau}(N,N_s)} = \frac{1}{\bar{\tau}_{rep}(N)} + \frac{1}{\bar{\tau}_{mod}(N,N_s)} \tag{5}$$

The results obtained for the four blends studied are listed in Table II. It shows that, in the shortest matrices, the reptation of the N chain is a negligible process and, in the largest matrices, the constraint release inducing a modification of the tube plays an important role in the relaxation of the N chain.

Figure 10 shows that the variation of $\bar{\tau}_{mod}(N,N_s)$ with molecular weight M_s of the matrix follows the law

$$\bar{\tau}_{mod}(N,N_s) \propto M_s^{2.3\pm0.1}$$

which is not the law predicted by Klein and Graessley. If constraint release is due to the motions of the chains of the matrix, the average time of modification of the tube is proportional to the relaxation time of the N_s chains and so, formally, $\bar{\tau}_{mod}(N,N_s) \propto M_s^{3.4}$, using the experimental exponent. The discrepancy could be related to the fact

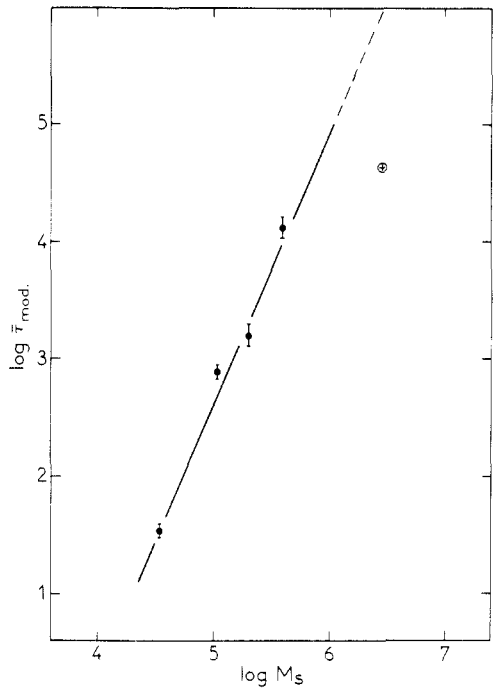

Figure 10. Average relaxation time for the tube modification of the F270 sample at $T = 160$ °C as a function of molecular weight of the matrix. (⊕) represents the relaxation time of the F270 fraction.

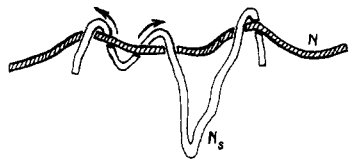

Figure 11. An N_s chain of the matrix could have several contacts with the N chain. Thus, constraint releases would be correlated and the average time of constraint release would be faster than if constraints were independent.

that the interactions between the N chain and the N_s chains of the matrix are connected. The motion of each constraint materializing the tube is connected to some neighbors and this correlation is all the more important as the matrix is constituted of larger chains. One of the processes of correlation could be the fact that one chain of the matrix has several contacts, as entanglements, with an N chain (Figure 11). The release of one constraint makes easier the release of neighboring constraints relative to the same N_s chain. Experimentally, we establish that $\bar{\tau}_{mod}(N,N_s) \propto \bar{\tau}_{rep}(N_s)/N_s$.

Figure 10 shows that, if we extend the straight line representing the variations of $\bar{\tau}_{mod}(N,N_s)$ vs. N_s, we obtain the value of $\bar{\tau}_{mod}(N)$ for a monodisperse sample corresponding to $N = N_s$. In our case, we can calculate this average time for the sample F270: $\bar{\tau}_{mod}(N) \simeq 10^6$ s. Comparing to the average reptation time for the same sample (last line in Table II), we verify that, for large chains in their own surroundings, the process of relaxation observed in the terminal region is only the reptation.

3. Influence of the Test Chain. Modifying the length of the N chain isolated in a given monodisperse matrix, we can try the assumption that compares the tube with a Rouse chain of N beads; thus, its relaxation time is proportional to N^2. We have used the F11 matrix in which we have blended the samples F39, F90, F120, F270, and F380 with a weight-concentration of 2%. Figure 12 shows that two separate domains of relaxation are observed, except for the sample F39, and thus we can determine

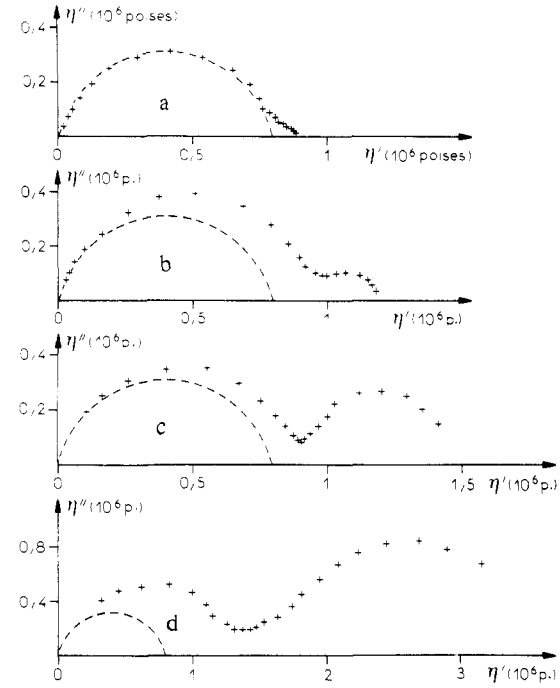

Figure 12. Complex viscosity at $T = 160$ °C deduced from the master curves of $G'(\omega)$ and $G''(\omega)$ for the blends listed in Table III ($\phi = 0.02$). The N chain is, from top to bottom, (a) F39, (b) F90, (c) F270, and (d) F380. The dashed arc of circle represents the behavior of the F11 fraction.

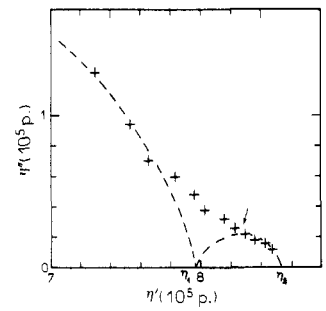

Figure 13. Low-frequency part of the curve of Figure 12a. The arrow indicates the frequency that defines the average relaxation time $\bar{\tau}(N,N_s)$.

Table III
Relaxation Times of N Chains in an N_s Matrix at 160 °C

N chain	N_s matrix	$\bar{\tau}(N,N_s)$, s	$\bar{\tau}_{mod}(N,N_s)$, s
F39	F11	2.0×10^1	2.9×10^1 [a]
F90	F11	1.45×10^2	1.7×10^2
F120	F11	4.0×10^2	4.2×10^2
F270	F11	7.8×10^2	7.95×10^2
F380	F11	3.55×10^3	3.65×10^3

[a] This value has been obtained by using relations 5 and 6.

$\bar{\tau}(N,N_s)$. For the four blends showing a well-defined low-frequency domain, we may derive the tube modification time $\bar{\tau}_{mod}(N,N_s)$ using eq 5, in which $\bar{\tau}_{rep}(N)$ is the same as the average relaxation time $\bar{\tau}(N)$ observed for the monodisperse N samples. For the blend F11–F39, the size of the low-frequency domain is much smaller than those of the high-frequency domain and thus we do not observe a maximum of η'' in the low-frequency part. Thus, we have determined $\bar{\tau}(N,N_s)$ in this case as the reciprocal of the frequency for $\eta' = \eta_1 + (\eta_2 - \eta_1)/2$. η_1 and η_2 represent the viscosities of the ends of the low-frequency domain. In Figure 13, that frequency is located at the end of the arrow. The results are listed in Table III, and Figure 14 shows

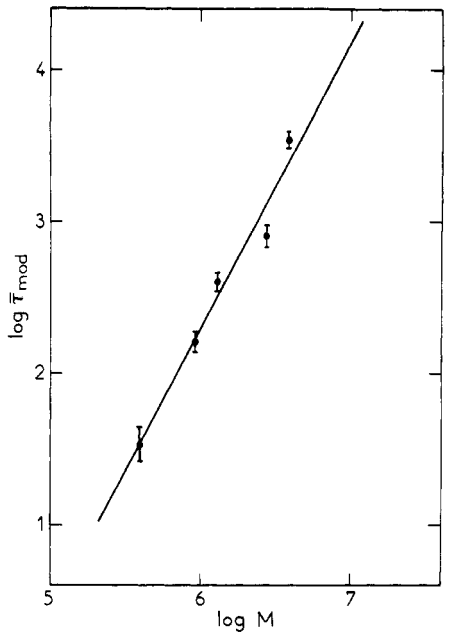

Figure 14. Average relaxation time for the tube modification of the N-chain samples at $T = 160$ °C as a function of molecular weight. Matrix is the F11 fraction.

that the variations of $\bar{\tau}_{mod}(N,N_s)$ vs. the molecular weight of the long chain follow the law

$$\bar{\tau}_{mod}(N,N_s) \propto M^{1.9\pm0.1}$$

Thus, it seems that one can really compare the tube to a Rouse chain for which the terminal relaxation times scales like M^2.

Using the results of the part above, we can write that, for an N chain (molecular weight M) isolated in a matrix of monodisperse N_s chains (molecular weight M_s), the average time of tube modification is

$$\bar{\tau}_{mod}(N,N_s) = (1.4 \pm 0.2) \times 10^{-21} M^{1.9} M_s^{2.3} \text{ s}$$

at $T = 160$ °C for polystyrene.

Thus, for a monodisperse sample

$$\bar{\tau}_{mod}(N) = (1.4 \pm 0.2) \times 10^{-21} M^{4.2} \text{ s}$$

and, using relation 4, in which the variations of $\bar{\tau}(N)$ are the experimental data (Figure 6), we obtain the values of $\bar{\tau}_{rep}(N)$ well depicted by the relation for $M \geq 390\,000$:

$$\bar{\tau}_{rep}(N) = 2.3 \times 10^{-17} M^{3.3} \text{ s} \quad (6)$$

We can see that the process of constraint release does not explain the discrepancy between the experimental coefficient ($\tau_{rep} \propto M^{3.4}$) and the theoretical exponent ($\tau_{rep} \propto M^3$).

This relation (6) has been used to deduce $\bar{\tau}_{mod}(N,N_s)$ for the blend F39–F11 (first line in Table III) because, for the narrow-distribution sample F39, the diffusion mechanisms include reptation and constraint release (for the F39 sample, $\bar{\tau}_{mead} = 40$ s and $(\bar{\tau}_{rep})_{calcd} = 65$ s). Therefore, the ratio $\bar{\tau}_{mod}(N)/\bar{\tau}_{rep}(N) \simeq 6 \times 10^{-5} M^{0.9}$ confirms that the process of constraint release is negligible for narrow-distribution samples of very long chains.

Our results are in agreement with measurements of self-diffusion coefficients for large labeled chains. They show that, if the matrix is made with chains larger than the labeled chains, the diffusion coefficient is roughly the same as that for labeled chains in their own surroundings.[25,26]

But, for the blends studied in this part of our work, the matrix is made with chains for which the process of constraint release influences their terminal relaxation ($\bar{\tau}_{mod}(N_s)/\bar{\tau}_{rep}(N_s) \simeq 2$ for sample F11). Thus, for those N_s chains, interactions with much larger N chains increase the tube modification time and also the relaxation time observed for the matrix. In Figure 12, the dashed line represents the behavior of the monodisperse F11 sample, and that relaxation domain is affected by the presence of large chains. This is demonstrated particularly for the blend F11–F380. Its amplitude is increased and the average relaxation time also. This effect would be better seen for blends in which the concentration of large chains in the matrix is increased.

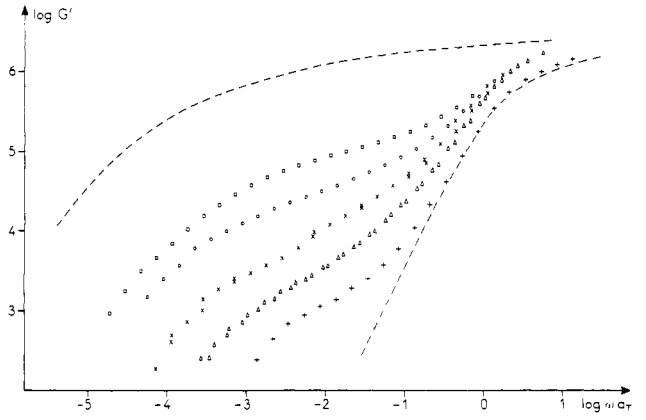

Figure 15. Master curves of storage modulus at $T = 160$ °C for blends F10–F270. The dashed lines represent the behavior of the two components alone. Experimental points correspond, from left to right, to $\phi = 0.31$, 0.20, 0.10, 0.05, and 0.02.

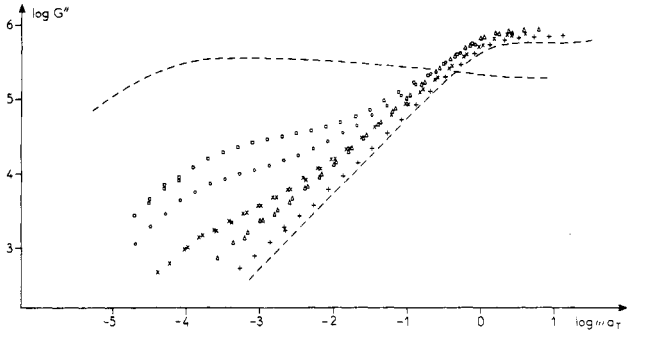

Figure 16. Master curves of loss modulus at $T = 160$ °C for the blends F10–F270. The curves have the same meaning as in Figure 15.

4. Influence of Concentration. We have assumed that, for the concentrations used in the previous blends ($C = 0.02$ g/g), the N chains were isolated in the matrix and we have neglected the N–N interactions. In order to demonstrate the effect of such interactions in the diffusion processes and, in particular, in the tube modification, we have made blends of samples F10 and F270, varying the concentration of sample F270 between 0.02 and 0.31 g/g. For the highest concentrations, it is impossible to reach the terminal region ($G' \propto \omega^2$ and $G'' \propto \omega$) and thus to determine the zero-shear parameters η_0 and J_e^0.

Using the master curves of Figures 15 and 16, we have calculated $\eta'(\omega)$ and $\eta''(\omega)$ and determined an average time $\langle\bar{\tau}(N,N_s)\rangle$ for the low-frequency relaxation, using the usual method. Thus, we have deduced an average time for the tube modification for the N chain: $\langle\bar{\tau}_{mod}(N,N_s)\rangle$ using relations 5 and 6. Results are reported in Table IV.

In order to discuss these results, it is necessary to take into account two types of interactions for an N chain: N–N interactions with a ratio ϕ, and N–N_s interactions with a ratio $1 - \phi$, ϕ being the weight fraction of the N chains. For each type of interaction, the mean waiting time for

Table IV
Rheological Properties of F10–F270 Binary Blends at 160 °C

ϕ	η_0, P	J_e^0, cm²/dyn	$\langle\bar{\tau}_{mod}(N,N_s)\rangle$, s	$\langle\bar{\tau}(N_s,N)\rangle$, s
0	5.75×10^5	1.26×10^{-6}		5.8×10^{-1}
0.02	1.05×10^6	1.78×10^{-4}	6.4×10^2	6.0×10^{-1}
0.05	2.51×10^6	4.00×10^{-4}	1.5×10^3	6.5×10^{-1}
0.10	1.00×10^7	3.00×10^{-4}	3.3×10^3	8.2×10^{-1}
0.20	5.75×10^7	9.55×10^{-5}	8.9×10^3	9.6×10^{-1}
0.31	2.09×10^8	5.00×10^{-5}	3.2×10^4	9.9×10^{-1}
1	1.59×10^{10}	3.16×10^{-6}	1.2×10^6	

constraint release is obtained by using the function $F(t)$, which represents the initial fraction of steps still occupied at time t for each neighboring chain. If we assume that the equation of $F(t)$ proposed by Graessley[8] may be used with an average relaxation time, then for N–N interactions

$$F_N(t) = \frac{\pi^2}{12} \exp\left(-\frac{\Lambda_{(z)}t}{\bar{\tau}_w(N)}\right) \quad (7)$$

where z is the average number of suitable constraints per cell, and, for the N–N_s interactions

$$F_{N_s}(t) = \frac{\pi^2}{12} \exp\left(-\frac{\Lambda_{(z)}t}{\bar{\tau}_w(N_s)}\right) \quad (8)$$

Then we deduce a function $F(t)$ which represents the average fraction of initial steps still occupied by a chain neighboring an N chain, whatever this length

$$F(t) = \phi F_N(t) + (1 - \phi)F_{N_s}(t) \quad (9)$$

which allows us to define an average waiting time for constraint release for an N chain in the same way as Graessley:[8]

$$\langle\bar{\tau}_w(N,N_s)\rangle = \int_0^{+\infty} [F(t)]^z \, dt \quad (10)$$

Using experimental results of parts II-2 and II-3, we obtain an average relaxation time for modification of the tube:

$$\langle\bar{\tau}_{mod}(N,N_s)\rangle \propto M^{1.9}\langle\bar{\tau}_w(N,N_s)\rangle$$

$\langle\bar{\tau}_w(N,N_s)\rangle$ may be calculated with the expressions (7), (8) (in which $\bar{\tau}_w(N) \propto M^{2.3}$ and $\bar{\tau}_w(N_s) \propto M_s^{2.3}$), (9), and (10), choosing a value for z.

We have tried several values of z, and Figure 17 shows a good agreement between the experimental results and the curve obtained for $z = 3$, corresponding to the expression

$$\langle\bar{\tau}_{mod}(N,N_s)\rangle = \bar{\tau}_{mod}(N,N_s)\phi^3\left[\frac{1}{\alpha} + 9\left(\frac{1-\phi}{\phi}\right) \times \left(\frac{1}{1+2\alpha}\right) + 9\left(\frac{1-\phi}{\phi}\right)^2\left(\frac{1}{2+\alpha}\right) + \left(\frac{1-\phi}{\phi}\right)^3\right] \quad (11)$$

with

$$\alpha = (M_s/M)^{2.3}$$

This relation can be simplified, if $\alpha \ll 1$, in the form

$$\langle\bar{\tau}_{mod}(N,N_s)\rangle = \bar{\tau}_{mod}(N,N_s)\phi^3\left[\left(\frac{M}{M_s}\right)^{2.3} + 9\left(\frac{1-\phi}{\phi}\right) + \frac{9}{2}\left(\frac{1-\phi}{\phi}\right)^2 + \left(\frac{1-\phi}{\phi}\right)^3\right] \quad (12)$$

This indicates that, according to Graessley's model, there are three suitable constraints per cell. If every constraint corresponds to an entanglement, the number N of steps would be $N = M/3M_e$.

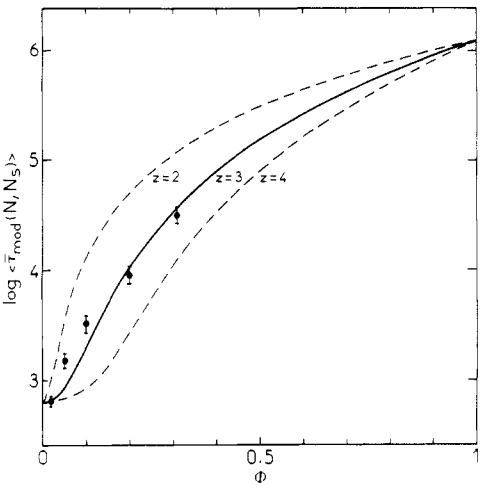

Figure 17. Average relaxation time for the tube modification of the N chains in the blends F10–F270 as a function of weight fraction ϕ at 160 °C. Full line corresponds to eq 12.

Figure 17 shows that $\langle\bar{\tau}_{mod}(N,N_s)\rangle$ for $\phi = 0.02$ is very close to the tube modification time for an N chain perfectly isolated ($\phi \to 0$). Thus, for the concentration used to show the influence of the lengths of the matrix and the N chain ($\phi = 0.02$), the N chain had a behavior of the individual chain.

In the same way as the composition of the blend modifies the terminal relaxation times for the larger N chain, the matrix of shorter N_s chains exhibits an increase of its relaxation times when the ratio of large chains increases. Figure 15 and 16 show that the high-frequency region is shifted toward low frequencies as ϕ increases. It seems that the curves reach a maximal shift corresponding to a maximal increase of the relaxation time when $\Delta \log \bar{\tau} \simeq 0.3$.

If we consider that the average relaxation time for tube modification of the N_s chains follows the same law as the N chain, then (for $(M/M_s)^{2.3} \gg 1$)

$$\langle\bar{\tau}_{mod}(N_s,N)\rangle = \bar{\tau}_{mod}(N_s)\phi^3\left[\left(\frac{M}{M_s}\right)^{2.3} + 9\left(\frac{1-\phi}{\phi}\right) + \frac{9}{2}\left(\frac{1-\phi}{\phi}\right)^2 + \left(\frac{1-\phi}{\phi}\right)^3\right] \quad (13)$$

Using this expression, we may calculate $\langle\bar{\tau}_{mod}(N_s,N)\rangle$ and thus the relaxation time $\langle\bar{\tau}(N_s,N)\rangle$ from the relation

$$\langle\bar{\tau}(N_s,N)\rangle^{-1} = \langle\bar{\tau}_{rep}(N_s)\rangle^{-1} + \langle\bar{\tau}_{mod}(N_s,N)\rangle^{-1}$$

with $\bar{\tau}_{rep}(N_s) \simeq 1$ s calculated for the monodisperse F10 sample.

The results presented in the last column of Table IV show that, for a concentration of the N chain higher than 0.20, the relaxation time of the N_s chains is similar to the reptation time and so the maximum shift for that time is $\log(\bar{\tau}_{rep}(N_s)/\bar{\tau}(N_s)) = 0.24$, close to the experimental shift.

The effect of the concentration of large chains in the blend appears in the breadth of the relaxation time distribution. We have indicated that, on the curves representing η'' as a function of η', the angle β is a measure of that breadth (Figure 4). In particular, β is zero for a unique relaxation time. For the blends F10–F270, we have determined the angle β of the low-frequency domain, and Figure 18 shows the variations of the parameter $1 - \tan\beta$, which is the dispersion parameter for a Cole–Cole distribution.[18] For high concentrations of N chains, the

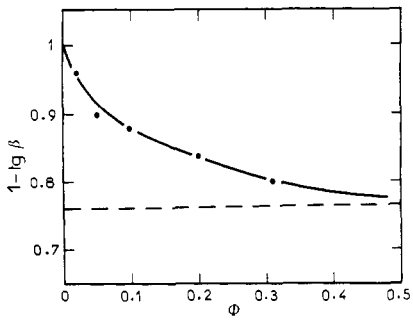

Figure 18. Dispersion parameter of relaxation time distribution for sample F270 in blends F10–F270 as a function of F270 weight fraction.

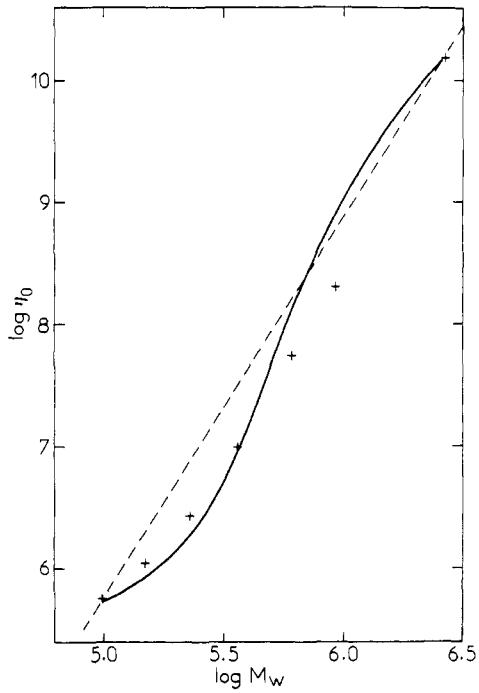

Figure 19. Zero-shear viscosity for blends F10–F270 as a function of weight molecular weight at T = 160 °C. The full line corresponds to eq 14.

dispersion parameter reaches the same value as for a monodisperse sample and, when the concentration tends to zero, it seems that the low-frequency relaxation exhibits a unique relaxation time. For the lowest concentration studied (ϕ = 0.02), the N chain has been considered as isolated—no N–N interactions—so the mean waiting time $\bar{\tau}_w(N,N_s)$ is the same for all constraints, leading to a unique relaxation time for the tube modification process. A small polydispersity leads to a small dispersion of relaxation times. When the N–N interactions become efficient, there are correlated motions of the N chains and thus the relaxation times are distributed, independently of the molecular weight distribution. Then it seems that, even for a sample strictly monodisperse, the correlated motions of the chains, including reptation, constraint release, and other mechanisms, induce a distribution of relaxation times.

The zero-shear viscosity η_0 and the steady-state compliance J_e^0 vary with concentration. For the blends F10–F270, the compliance J_e^0 follows the usual variations: it reaches rapidly a maximum value for a concentration of about 5% but the viscosity η_0 does not follow the usual power law $\eta_0 \propto M_w^{3.4}$. Figure 19 shows that the experimental points are below the dashed line representing the power law. This observation is unusual but, to our knowledge, binary blends with components so different

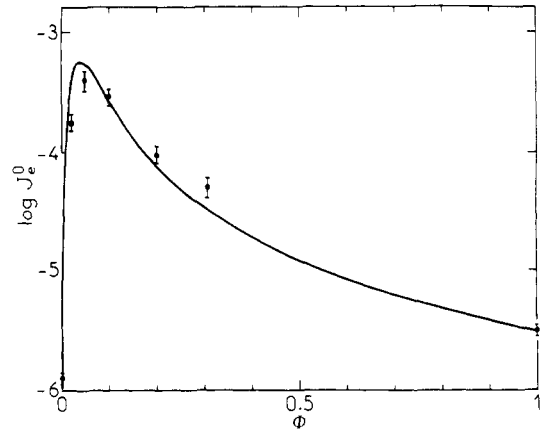

Figure 20. Steady-state recoverable compliance for blends F10–F270 as a function of F270 weight fraction. The full line corresponds to eq 15.

(M/M_s = 27) have not been studied. Our results can be explained, at least qualitatively, as an effect of constraint release.

Some blending laws have been given[27,28] to represent the behavior of binary blends of entangled molecules. These quadratic laws define the relaxation time distribution function $H(\tau)$ for the blend as the sum of three terms: the function $H_1(\tau)$ and $H_2(\tau)$ of each component and a coupling term due to the interactions between the two components. Using a molecular approach, Graessley[28] deduces the following expressions for the limiting parameters:

$$\eta_0 = \eta_{0N}(\phi^2 + d_1\phi(1-\phi) + R(1-\phi)^2)$$

$$J_e^0 = J_{eN}^0 \frac{\phi^2 + d_2\phi(1-\phi) + R^2(1-\phi)^2}{[\phi^2 + d_1\phi(1-\phi) + R(1-\phi)^2]^2}$$

where $R = (M/M_s)^{3.5}$ and d_1 and d_2 are parameters related to the molecular structure of the polymer.

These expressions account only qualitatively for the experimental results and lead to too high values.

Assuming that the tube modification represents an interchain coupling, we suggest writing

$$\eta_0 \propto \phi^2\langle\bar{\tau}(N,N_s)\rangle + (1-\phi)^2\langle\bar{\tau}(N_s,N)\rangle \qquad (14)$$

with

$$\langle\bar{\tau}(N,N_s)\rangle^{-1} = \langle\bar{\tau}_{rep}(N)^{-1}\rangle + \langle\bar{\tau}_{mod}(N,N_s)\rangle^{-1}$$

and

$$\langle\bar{\tau}(N_s,N)\rangle^{-1} = \langle\bar{\tau}_{rep}(N_s)\rangle^{-1} + \langle\bar{\tau}_{mod}(N_s,N)\rangle^{-1}$$

The full line on Figure 19 shows that, for the low values of concentration, relation 14 leads to values of viscosity lower than those of the power law. But, for the high values of concentration, there is a discrepancy between experimental data and values from relation 14.

In the same way, we propose the following expression for the steady-state compliance:

$$J_e^0 \propto \frac{\phi^2\langle\bar{\tau}(N,N_s)\rangle^2 + (1-\phi)^2\langle\bar{\tau}(N_s,N)\rangle^2}{[\phi^2\langle\bar{\tau}(N,N_s)\rangle + (1-\phi)^2\langle\bar{\tau}(N_s,N)\rangle]^2} \qquad (15)$$

in which the average relaxation times of the two components in the blend include the effects of interchain couplings. The curve obtained from relation 10 is in good agreement with experimental results, in particular for the value of the maximum of J_e^0, which is a few hundred times the compliance of each component (Figure 20).

In the two relations (14) and (15), the coefficient of proportionality is adjusted to fit the curves and the experimental data for the two components alone.

In summary, it seems that the mechanism of constraint release plays an important role in the terminal viscoelastic properties of binary blends that are a first example of a polymer with a broad molecular weight distribution. But the contribution of this process to the diffusion of any chain in surroundings of chains with different lengths has to be further studied.

Conclusion

Using a classical technique of mechanical analysis, dynamic shear measurements in the terminal region, and using binary blends of monodisperse linear polystyrene with very different molecular weights, we have demonstrated the effects of constraint release in the diffusion motion of entangled chains. We have shown that the relaxation times typical of this mechanism follow partly the scaling laws given by Klein[3] and Graessley[8] for an N chain isolated in a matrix of N_s chains. It seems that we can consider the tube of the reptation models as a Rouse chain with a characteristic time $\bar{\tau}_{mod}(N,N_s) \propto N^2$ but the mean waiting time for a constraint release is not directly related to the reptation time of the N_s chains and we have observed that $\bar{\tau}_w \propto \bar{\tau}_{rep}(N_s)/N_s$, perhaps due to the fact that the topological constraints acting on an N chain are not independent, so they have correlated motions.

For binary blends in which the surroundings of an N chain is constituted with N chains and N_s chains, we have related the characteristic time of tube modification with concentration. Thus, we have determined that a cell in the Graessley model contains three constraints that can release, involving a local modification of the primitive path. This mechanism, combined with the reptation motion in the quadratic blending laws, allowed us to describe reasonably the variations of the steady-state compliance J_e^0 and qualitatively those of the zero-shear viscosity η_0. In order to improve the given model, it would be necessary to take into account possible correlations between the two motions of diffusion: diffusion of one chain along its own contour and modification of the tube constituted by the neighboring chains and perhaps other mechanisms like the path length fluctuations considered by Graessley[8] and Doi.[29]

We have used polystyrene, for which monodisperse samples are available on the market, but this polymer shows two drawbacks: the terminal and plateau relaxations are not clearly separated and so the master curves of $G''(\omega)$ do not exhibit a maximum which allows one to define the plateau modulus G_N^0 and thus the average time $\bar{\tau}_n$; on the other hand, the critical molecular weight M_c above which one considers the entanglement effects is high ($M_c \simeq 35\,000$) and a good study with high molecular weights is not possible for $M/M_c > 100$. We have shown that the mechanism of constraint release plays the leading part when the N chain is much larger than the matrix ($M/M_s > 5$ approximately) and so the number of M–M_s pairs is reduced. For these reasons, it seems that other polymers are better for the study that we just made, and they would allow a test of the results of the present work. In particular, using matrices of short chains strongly entangled, one could verify whether the experimental result $\bar{\tau}_{mod}(N,N_s) \propto M_s^{2.3}$ is not due merely to the fact that the matrix has not reached its asymptotic behavior.

Registry No. Polystyrene, 9003-53-6.

References and Notes

(1) de Gennes, P.-G. *J. Chem. Phys.* **1971**, *55*, 572.
(2) Doi, M.; Edwards, S. F. *J. Chem. Soc., Faraday Trans. 2* **1978**, *74*, 1789, 1802, 1818; **1979**, *75*, 38.
(3) Klein, J. *Macromolecules* **1978**, *11*, 852.
(4) Graessley, W. W. *J. Polym. Sci., Polym. Phys. Ed.* **1980**, *18*, 27.
(5) Kan, H. C.; Ferry, J. D.; Fetters, L. J. *Macromolecules* **1980**, *13*, 1571.
(6) Taylor, C. R.; Kan, H. C.; Nelb, G. W.; Ferry, J. D. *J. Rheol.* **1981**, *25*, 507.
(7) Granick, S.; Pedersen, S.; Nelb, G. W.; Ferry, J. D.; Macosko, C. W. *J. Polym. Sci., Polym. Phys. Ed.* **1981**, *19*, 1745.
(8) Graessley, W. W. *Adv. Polym. Sci.* **1982**, *47*, 67.
(9) Daoud, M.; de Gennes, P.-G. *J. Polym. Sci., Polym. Phys. Ed.* **1979**, *17*, 1971.
(10) Ferry, J. D. "Viscoelastic Properties of Polymers", 3rd ed.; Wiley: New York, 1980.
(11) Plazek, D. J.; Chelko, A. J. *Polymer* **1977**, *18*, 15.
(12) Fuoss, R. M.; Kirkwood, J. G. *J. Am. Chem. Soc.* **1941**, *63*, 385.
(13) Williams, M. L.; Ferry, J. D. *J. Polym. Sci.* **1953**, *11*, 169.
(14) Ninomiya, K.; Ferry, J. D. *J. Colloid. Sci.* **1959**, *14*, 36.
(15) Tschoegl, N. W. *Rheol. Acta* **1971**, *10*, 582.
(16) Marin, G.; Montfort, J. P.; Arman, J.; Monge, Ph. *Rheol. Acta* **1979**, *18*, 629.
(17) Marin, G. Thèse d'Etat, Université de Pau, 1977.
(18) Cole, K. S.; Cole, R. H. *J. Chem. Phys.* **1941**, *9*, 341.
(19) Graessley, W. W. *Adv. Polym. Sci.* **1974**, *16*, 1.
(20) Graessley, W. W.; Edwards, S. F. *Polymer* **1981**, *22*, 1329.
(21) Raju, V. R.; Menezes, E. V.; Marin, G.; Graessley, W. W.; Fetters, L. J. *Macromolecules* **1981**, *14*, 1668.
(22) Marin, G.; Labaig, J. J.; Monge, Ph. *Polymer* **1975**, *16*, 223. Montfort, J. P. *Ibid.* **1976**, *17*, 1054.
(23) Jamieson, M.; Telford, D. *Macromolecules* **1982**, *15*, 1329.
(24) de Gennes, P.-G. "Scaling Concepts in Polymer Physics"; Cornell University Press: Ithaca, NY, 1979; p 59.
(25) Leger, L.; Hervet, H.; Rondelez, F. *Macromolecules* **1981**, *14*, 1732.
(26) Klein, J. *Macromolecules* **1981**, *14*, 460.
(27) Bocue, D. C.; Masuda, T.; Einaga, Y.; Onogi, S. *Polym. J.* **1970**, *1*, 563.
(28) Graessley, W. W. *J. Chem. Phys.* **1971**, *54*, 5143.
(29) Doi, M. *J. Polym. Sci., Polym. Lett. Ed.* **1981**, *19*, 265.
(30) Plazek, D. J.; O'Rourke, V. M. *J. Polym. Sci., Part A-2* **1971**, *9*, 209.